Clays and Clay Minerals, Vol. 56, No. 1, 10–22, 2008.

CATION MASS-VALENCE SUM (CM-VS) APPROACH TO ASSIGNING OH-BENDING BANDS IN DIOCTAHEDRAL SMECTITES

WILL P. GATES

Department of Civil Engineering, Monash University, Clayton VIC3800, Australia

Abstract—The assignments of OH-bending bands in the infrared (IR) spectra of dioctahedral smectites (montmorillonites, ferruginous smectites, and nontronites) have been revisited using a cation mass-valence sum (CM-VS) approach to quantify octahedral cation occupancy. The CM-VS approach enabled prediction of OH-bending band positions (in wavenumbers) related to OH-sharing octahedral cation pairs that had valence sums of 4 and 5, and cation masses associated with Fe(II) and Mg. Application of rules for the relationship enabled determination of the location of OH-sharing octahedral cation pairs containing Mg and Fe(II) for which previous assignments have been considered controversial, *e.g.* Fe(III)Mg-OH and MgMg-OH, or for which assignments have been missing due to lack of spectroscopic evidence, *e.g.* AlFe(II)-OH, Fe(III)Fe(II)-OH, Fe(II)Mg-OH, and Fe(II)Fe(II)-OH. Examples of these bands from several natural ferruginous smectites and nontronites are discussed. Quantification of IR spectra was used to develop a better understanding of the octahedral cation occupancy of this important class of Fe(III)-enriched smectites. While Fe(II) contents may be somewhat overestimated by the IR technique, those for four of the six ferruginous smectites studied here agree well with data from Mössbauer spectroscopy.

Key Words—Cation Mass, Cation Pairs, Infrared Spectroscopy, Octahedral, Smectite Chemistry, Valence Sum.

INTRODUCTION

Infrared spectroscopy is useful as a probe for structural chemistry because all OH-sharing octahedral cation pairs contribute to the IR absorption spectrum. Quantitative application of IR spectroscopy to the structural analysis of smectites (Slonimskayá *et al.*, 1986; Madejová *et al.*, 1994; Bishop *et al.*, 1999; Vantelon *et al.*, 2001; Gates *et al.*, 2002; Petit *et al.*, 2002) generally provides useful and accurate accessory information as long as care is taken in ensuring pure samples and accurate analytical data. In general, the uptake of this method has been in part hampered by lack of unambiguous assignments of some absorption bands.

Recently, Martinez-Alonso *et al.* (2002) and Botella *et al.* (2004) used molecular modeling techniques to calculate vibrational frequencies for IR bands in dioctahedral smectites. Some of the estimates made were for various OH-sharing octahedral cation pairs for which insufficient spectroscopic data exist: *e.g.* AlFe(II)-OH, Fe(III)Fe(II)-OH, Fe(II)Mg-OH, and Fe(II)Fe(II)-OH bending bands. Only a few spectroscopic studies have been conducted on reduced smectites (Stucki and Roth, 1976; Komadel *et al.*, 1995; Fialips *et al.*, 2002a, 2002b; Lee *et al.*, 2006) and assignments for these mixed-valence cation pairs have been difficult to assess, presumably due to de-hydroxylation and proton-exchange reactions that take place in the solid state (Lear and Stucki, 1985; Heller-Kellai, 1997; Drits and Manceau 2000). The ability to assign Fe(II) bands in the IR spectra may prove useful given the increased research interest in mineral-microbial interactions (Dong *et al.*, 2003; Kim *et al.*, 2004; Stucki and Kostka, 2006).

Recent Mössbauer spectroscopic evidence (Thompson *et al.*, 2007; Cashion *et al.*, 2008) reveals minor amounts of Fe(II) in some of the ferruginous smectites studied by Gates (2005). This provides an opportunity to make assignments of IR bands associated with Fe(II) and to quantify the amount of Fe(II) in these same smectites. In the present work, IR spectra from Gates (2005) are re-fitted to investigate the possible evidence for the existence of OH-sharing Fe(II) and Mg bands.

IR band-assignment rules

The vibrational frequencies of OH (υ_{OH}) are related to the O–H force constant (k_{OH}) and the reduced mass (μ_{OH}) of the vibrating dipole through

$$\nu_{OH}(cm^{-1}) = \frac{1}{2\pi c}\left(\frac{k_{OH}}{\mu_{OH}}\right)^{\frac{1}{2}} \quad (1)$$

The force constant depends on the valence of cations directly bonded to OH: a decrease in their combined charge strengthens the bonding between the oxygen and proton and leads to increased vibrational frequency. The reduced mass has a negative effect in that a dipole of large mass will vibrate at a lower frequency. Besson and Drits (1997a, 1997b) showed that the position of OH-stretching bands in micas was dependent on a combina-

* E-mail address of corresponding author:
gateswp@smectech.com.au
DOI: 10.1346/CCMN.2008.0560102

tion of the valence sum and cation mass of the OH-sharing, *cis* occupying, octahedral cations. The cation mass (CM) is defined here as the sum of the mass ($m_M + m_N$) of cations M and N bonded to OH and the valence sum (VS) as the sum of their valences. Note that the cation mass used here differs from the classical reduced mass ($\mu_{OH} = m_1 \times m_2/(m_1 + m_2)$) of the entire vibrating dipole (*e.g.* $m_1 = M{-}O{-}N$, $m_2 = H$).

A review of the literature on OH stretching assignments in *trans*-vacant micas found that Besson and Drits (1997a, 1997b) identified the following rules:

(1) For OH-sharing cation pairs with the same VS, increases in CM result in decreases in the frequency of the vibration.

(2) For OH-sharing cation pairs of the same CM, increases in VS result in increases in the frequency of the vibration.

(3) Simultaneous increases in both CM and VS of OH-sharing cation pairs result in increased frequency of the vibration due to the larger effect of VS.

According to rule 1 above, the vibrational frequency of OH-sharing AlFe(III) pairs should be greater than OH-sharing Fe(III)Fe(III) pairs, because while their VS remains the same at 6, CM is greater in Fe(III)Fe(III) (~112 g mol^{-1} – ignoring the mass of O and H) than in AlFe(III) (~83 g mol^{-1}). According to rule 2, the Fe(III)Fe(III) group should have OH bands at higher frequency than the Fe(III)Fe(II) group. An OH band of Fe(III)Fe(III) should vibrate at higher frequency than one of Fe(III)Mg, as described by rule 3. These rules are shown in the present study to be generally applicable to the bending region of the IR, and specifically to both *cis*- and *trans*-vacant smectites.

Using previous band assignments for dioctahedral smectites (Gates, 2005), one can plot a CM-VS *vs.* wavenumber relationship for the OH-bending vibrations as shown in Figure 1, which shows that increased CM (*e.g.* from AlAl to Fe(III)Fe(III)) causes the OH-bending band position to shift to a lower wavenumber, but also that increased VS (*e.g.* from AlMg to AlAl, or from Fe(III)Mg to Fe(III)Fe(III)) causes the OH-bending band to shift to higher wavenumbers. For simultaneous differences in both CM and VS, *e.g.* AlMg to AlFe(III) or Fe(III)Mg to AlFe(III) or Fe(III)Fe(III), the OH-bending band position will be at a lower wavenumber for the OH-sharing cation pair with the lowest VS.

Prediction of band position and quantification of site occupancy

Besson and Drits (1997b) showed that the equation

$$M^aN^b - \mathrm{OH}(\mathrm{cm}^{-1}) = \frac{\left[M^aM^a - \mathrm{OH}(\mathrm{cm}^{-1}) + N^bN^b - \mathrm{OH}(\mathrm{cm}^{-1})\right]}{2} \quad (2)$$

can be used to predict the vibrational frequencies of any band corresponding to any mixture of cations and valence, provided that frequencies of like-cation pairs are known. Here, M and N are cations of different atomic mass with valences a and b, respectively.

Gates (2005) showed that quantification of octahedral site occupancy from IR data could be achieved with reasonable agreement with structural formula calculations based on crystal chemistry for 35 smectites. An equation for di-octahedral sheets in general form is

$$OctM^a = 4 \times \left[2 \times A(M^aM^a - \mathrm{OH}) + \sum_n A(M^aN^b - \mathrm{OH})\right] \quad (3)$$

Here $OctM^a$ is the number of sites per unit-cell occupied by the octahedral cation M of interest having valance a; N^b represents any other cation of any other valence that shares at least one OH along an edge with cation M^a; n is the number of M^aN^b-OH bands observed in the IR spectrum and A is the normalized integrated peak area of the IR band in question. Equation 3 will be applied below to recalculate structural formulae of some ferruginous smectites based on reinterpretation of IR spectra.

MATERIALS AND METHODS

The identities of the montmorillonite, ferruginous smectite, and nontronite samples and their preparation and analysis were as described by Gates *et al.* (2002) and Gates (2005). Briefly, the <0.2 μm fractions were collected from suspensions of Na-saturated material using centrifugation. Ferruginous smectite and nontro-

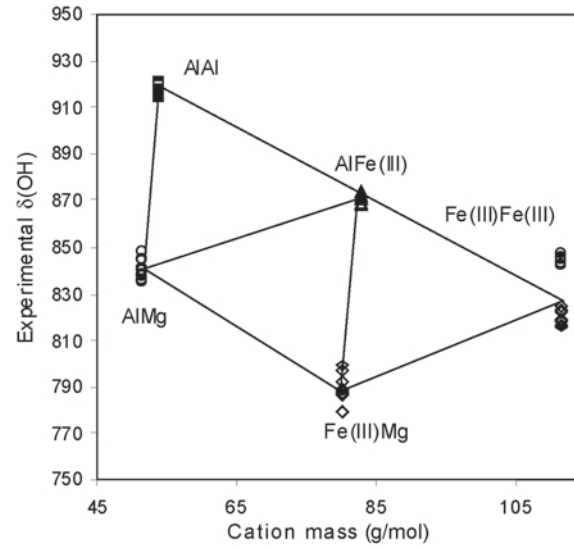

Figure 1. Cation mass-valence sum *vs.* wavenumber relationship for OH-sharing octahedral cation-pair bending bands in 35 smectites. Points represent the positions and assignments for 35 smectites studied by Gates (2005). Two sets of Fe(III)Fe(III)-OH bands exist in dioctahedral smectites, depending on octahedral Fe(III) content.

nite samples were often found to contain ferric oxide and/or kaolin impurities which are known to impact on structural formula calculations (Čícel *et al.*, 1992; Komadel *et al.*, 1993; Lear *et al.,* 1988; Gates *et al.*, 2002) and subsequently these were Li-saturated, redispersed, and the <0.1 mm fractions were collected. All samples were checked by X-ray diffraction (XRD) (Figure 2) and IR to ensure purity (Gates, 2005). The XRD and IR show that the samples are free of other common admixtures.

Sample preparation and diffuse reflectance infrared transform (DRiFT) spectra were collected as described by Gates (2005). Diffuse reflectance spectroscopy was performed on Ca^{2+}-saturated dry powders diluted (10 wt.%) in KBr. Spectra were collected on a Biorad FTS 175C Fourier transform spectrophotometer having an extended KBr beamsplitter and DTGS detector. As many as 512 acquisitions were co-added using the Kubelka-Monk formalism with a resolution of 2 cm^{-1}. Spectra processing – baseline correction and conversions – was done using Grams 32/AI (Galactic NH) software. Decomposition of spectra in the OH-bending region was carried out as described by Vantelon *et al.* (2001) and Gates (2005) to account for the intensity of the Si–O stretching bands. Voigtian envelopes were used to fit peak shape and all parameters were allowed to vary unconstrained once a suitable minimum was established.

RESULTS AND DISCUSSION

The octahedral cation-hydroxyl absorption bands in the 950–600 cm^{-1} region of the IR spectrum are relatively well resolved, and the intensity of each band

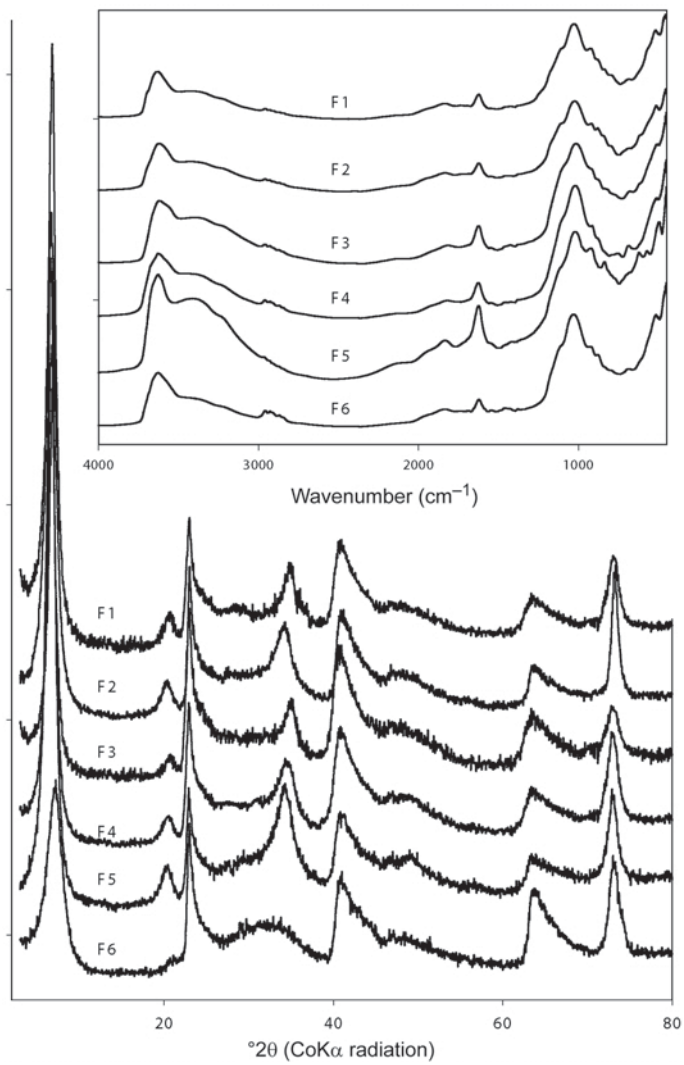

Figure 2. XRD traces and IR spectra (inset) of six ferruginous smectites studied here. F1 = Andamooka smectite, F2 = Redhill smectite, F3 = Nibost smectite, F4 = Drayton smectite, F5 = Mount Binjour Green smectite, F6 = Hroznetin smectite.

changes in a general fashion with chemical composition (Gates, 2005), but only by a few wavenumbers (Figure 1). These results provide an internally consistent check on the applicability of equation 2 to this region of the IR spectra of smectites.

Figure 1 can be extended to include other possible OH-sharing cation pairs. Extension of the left-most vertical line, which connects the positions of AlAl-OH bands to those for AlMg-OH (CM ≈ 49), to the point where it crosses an extension of the line connecting Fe(III)Fe(III) to Fe(III)Mg, forms a triangle, which itself can be divided into four equal parts. The new point, corresponding to VS = 4 and CM ≈ 49, represents MgMg-OH cation pair at ~760 cm^{-1}. Gates (2005) observed that most ferruginous smectites had absorption bands in the region 700–800 cm^{-1}, which as will be shown below, may be related to such VS = 4 cation pairs. The position of the new point for MgMg OH-sharing cation pairs is the intersection of values derived from the application of equation 1 for AlAl and AlMg and Fe(III)Fe(III) and Fe(III)Mg OH-sharing cation pairs: 770 cm^{-1} for montmorillonites, 757 cm^{-1} for ferruginous smectites, and 755 cm^{-1} for nontronites (Table 1).

Figure 1 can be further extended to include values of VS = 4 for Fe(II)Mg (CM ≈ 81) and Fe(II)Fe(II) (CM ≈ 112), and VS = 5 for AlFe(II) (CM ≈ 83) and Fe(III)Fe(II) (CM ≈ 112) cation pairs. We know that the Fe(III)Fe(III) to Fe(III)Fe(II)-OH to Fe(II)Fe(II) OH-sharing cation pairs should be along a vertical line at CM ≈ 112, but we do not know the exact cm^{-1} position of these bands. However, all of these positions (Figure 3) can be estimated with confidence in the following way.

First, the position of AlFe(II)-OH (VS = 5, CM ≈ 83) must be at lower cm^{-1} than that for AlMg-OH, because of the frequency-depressing effect of greater cation mass, but greater than that for Fe(III)Mg-OH, because of simultaneous changes in valence of the cations involved. The differences between the position of AlFe(II)-OH and these two bands should decrease and increase from montmorillonite to nontronite, respectively, because of the large change in position of these bands as a function of Fe content (Table 1). The line extending down from AlFe(III)-OH (CM ≈ 83) towards Fe(II)Mg-OH (CM ≈ 80) should have a slope of about half of that connecting

Table 1. Position (wavenumbers) and assignments of bands in the OH-bending region of the IR spectra of dioctahedral smectites. Band assignments are based on current discussion. Equation 2 enabled the prediction of the positions of bands associated with Fe(II) and Mg.

Assignment	Mont-morillonite	Ferruginous smectite	Nontronite
	Wavenumber (cm^{-1})		
AlAl-OH	920	917	915
AlFe(III)-OH	872	870	868
AlMg-OH	845	837	835
Fe(III)Fe(III)-OH	822	818	817, 844
AlFe(II)-OH	818	816	816
Fe(III)Mg-OH	796	788	785
Fe(III)Fe(II)-OH	769	766	767
MgMg-OH	770	757	755
Fe(II)Mg-OH	743	736	736
Fe(II)Fe(II)-OH	716	715	717

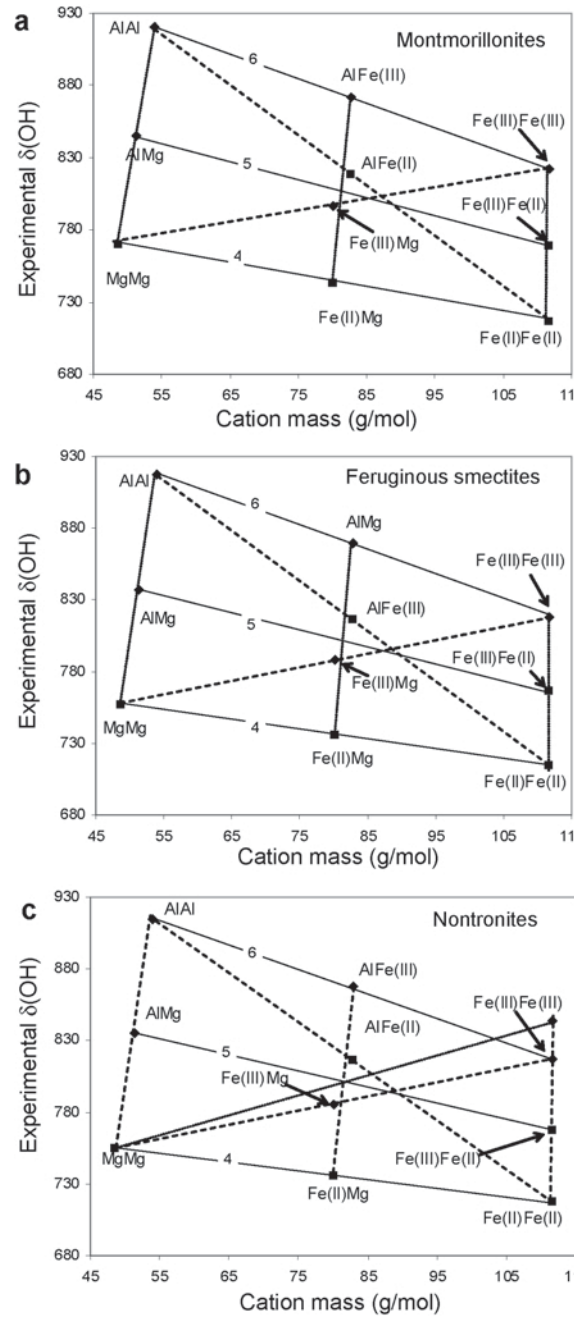

Figure 3. Cation mass-valence sum *vs*. wavenumber plot depicting experimental (diamonds) evidence for OH-bending bands containing Mg and Fe(II) as octahedral cations.

AlAl-OH (CM ≈ 54) with MgMg-OH (CM ≈ 49). The position of AlFe(II)-OH will thus be equidistant, but opposite from Fe(III)Mg-OH, of that line.

Second, projection of a line from AlMg-OH (CM ≈ 51) towards CM ≈ 112 will locate the position of Fe(III)Fe(II)-OH. Due to the effects of CM and VS, the slope of this VS = 5 line will be about half of the slope of the VS = 6 line, which extends from AlAl-OH to Fe(III)Fe(III)-OH, and it will pass through the average position of Fe(III)Mg-OH and AlFe(II)-OH (at CM ≈ 81.5). From the position of Fe(III)Fe(II)-OH, and that for Fe(III)Fe(III)-OH, positions of all Fe(II) containing OH-sharing cation pairs can now be predicted.

Finally, the Fe(II) bands (AlFe(II)-OH, Fe(III)Fe(II)-OH, Fe(II)Mg-OH, and Fe(II)Fe(II)-OH), as well as the MgMg-OH band, were iteratively adjusted from the known band positions (AlAl-OH, AlFe(III)-OH, AlMg-OH, Fe(III)Fe(III)-OH, and Fe(III)Mg-OH) for each smectite group: montmorillonite (Figure 3a), ferruginous smectite (Figure 3b), and nontronite (Figure 3c). The square data points in Figure 3 are those predicted using equation 2 and the diamonds are the average of data shown in Figure 1; their wavenumber values are also shown in Table 1.

In Figure 3, the values for VS = 6, 5, and 4 are each connected by solid lines corresponding to CM of various mixtures of Mg, Al, Fe(III), and Fe(II) cation pairs. Three nearly vertical dashed lines connect cation pairs with similar CM. Two dashed lines connect cation pairs having different VS and CM: from AlAl-OH through AlFe(II)-OH to Fe(II)Fe(II)-OH and from MgMg-OH through Fe(III)Mg-OH to Fe(III)Fe(III)-OH. The former series represents the resulting decrease in the wavenumber of the vibration with increased CM simultaneously with a decrease in valence sum. The latter series represents the case of simultaneous increases in both VS and CM, which result in an increased vibrational frequency. Note that the VS = 5 line passes by both AlMg-OH and Fe(III)Mg-OH at an intermediate position.

Gates (2005) showed that the position of many OH-bending bands changed proportionately with Fe(III) content, and that three distinct Fe(III)Fe(III)-OH bands existed that could be used to designate montmorillonite and beidellites, ferruginous smectites, and nontronites. For example, a band near 822 cm^{-1} is most commonly observed for montmorillonites and beidellites, but it shifts towards 818 cm^{-1} for ferruginous smectites and nontronites, and for nontronites a second band also appears at ~844 cm^{-1}. Thus, calculations were made separately for montmorillonites (Figure 3a), ferruginous smectites (Figure 3b), and nontronites (Figure 3c). In the present discussion, montmorillonites have <6.0% Fe_2O_3 (ignited basis) and thus include the real beidellites. Ferruginous smectites have >6%, but <27% Fe_2O_3 and usually have an Fe(III)Fe(III)-OH band near 820 cm^{-1}. Nontronites have >27% Fe_2O_3, and two Fe(III)Fe(III)-OH bending bands near 844 and 818 cm^{-1} (Gates, 2005; Gates *et al.*, 2002)

Spectroscopic evidence of Fe(II) bands in ferruginous smectites

Evidence of Fe(II) bands can be observed in the decomposed (Figure 4) IR spectra of Andamooka, Redhill, Nibost, Mount Binjour Green, and Hroznetin ferruginous smectites (F2, F3, F5, and F6 in Gates, 2005). The positions of OH-bending bands for cation pairs containing Fe(II) are given in Table 2 and Figure 5. Nibost and Mount Binjour Green smectites have similar chemistries of ~2Al, ~1Fe, and ~1Mg per unit-cell (Gates, 2005) and their IR spectra can be decomposed to contain a band near 816 cm^{-1} which Gates (2005) originally assigned to Fe(III)Fe(III)-OH. However, application of equation 2 shows that another possible assignment is AlFe(II)-OH for these smectites (Tables 1, 2). Note that Hroznetin smectite has a contribution near 818 cm^{-1}, which, as will be shown below, has to be assigned to Fe(III)Fe(III)-OH. For ferruginous smectites, the band near 818 cm^{-1} is likely to include contributions from both Fe(III)Fe(III)-OH and AlFe(II)-OH (Table 1).

All the ferruginous smectites show a broad absorbance encompassing 750−800 cm^{-1}, which can be decomposed into doublets with centers near 780−790 and 760−770 cm^{-1}. The higher wavenumber band can be confidently assigned to Fe(III)Mg-OH (Petit *et al.*, 2002; Gates, 2005), but the lower wavenumber band can be assigned to either Fe(III)Fe(II)-OH, MgMg-OH, or possibly Fe(II)Mg-OH (Figures 3, 4; Tables 1, 2). The band near 765−770 cm^{-1} for Andamooka, Redhill, Mount Binjour Green, and Hroznetin smectites can be confidently assigned to Fe(III)Fe(II)-OH. The IR spectrum of Andamooka, Redhill, Mount Binjour Green, and Hroznetin smectites can be decomposed to show a band

Table 2. Experimentally determined band positions for Fe(II) and Mg in ferruginous smectites.

Smectite	Band position (cm^{-1})	Assignment
Andamooka (F1)	772	Fe(III)Fe(II)-OH
	720	Fe(II)Fe(II)-OH
Redhill (F2)	770	Fe(III)Fe(II)-OH
	718	Fe(II)Fe(II)-OH
Nibost (F3)	816	AlFe(II)-OH
	758	MgMg-OH
Drayton (F4)	752	MgMg-OH
Mount Binjour Green (F5)	816	AlFe(II)-OH
	768	Fe(III)Fe(II)-OH
	755	MgMg-OH
	718	Fe(II)Fe(II)-OH
Hroznetin (F6)	765	Fe(III)Fe(II)-OH
	718	Fe(II)Fe(II)-OH

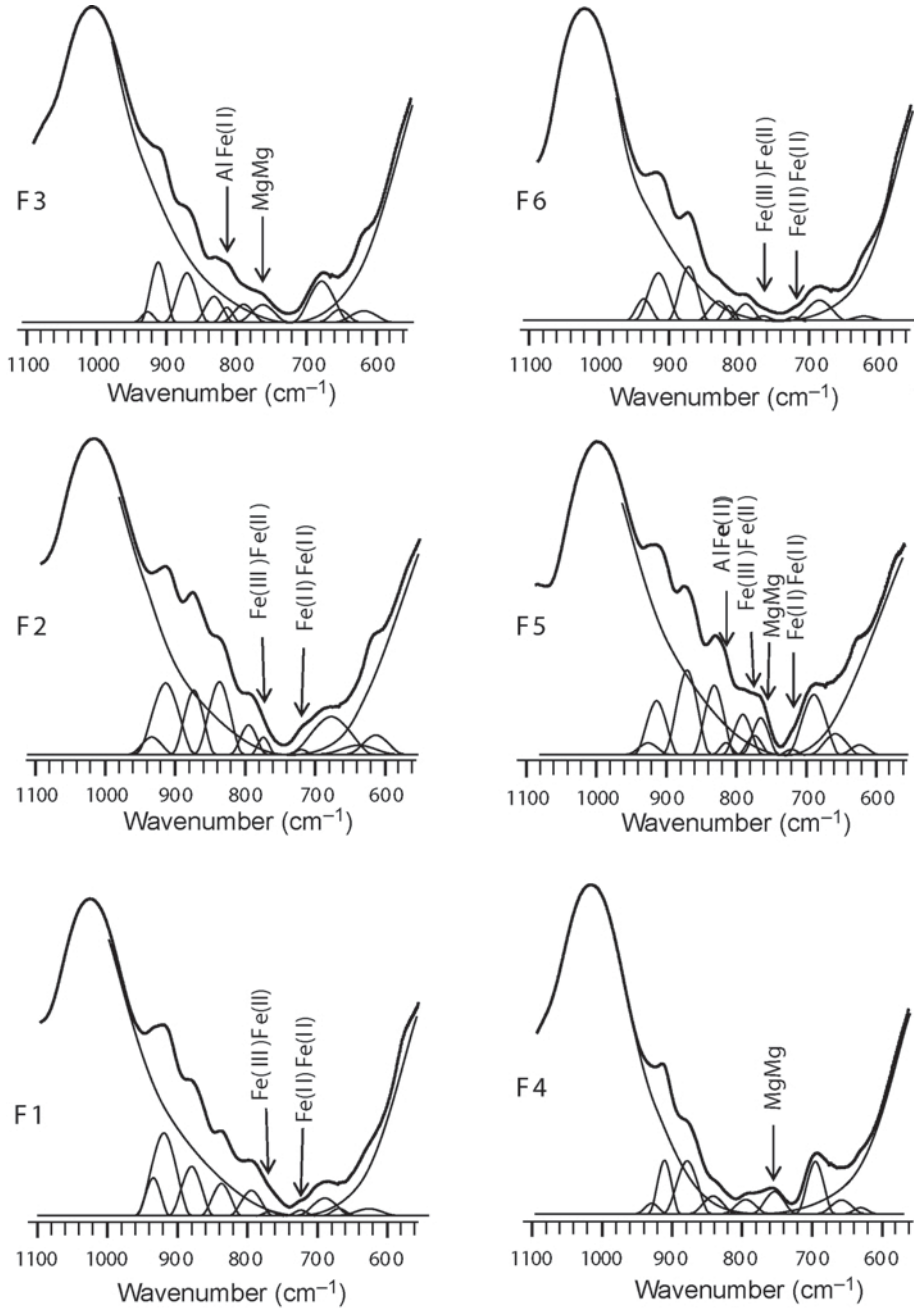

Figure 4. Decomposition of the OH-bending region of IR spectra of six natural ferruginous smectites with suspected Fe(II) and Mg bands. F1 = Andamooka smectite, F2 = Redhill smectite, F3 = Nibost smectite, F4 = Drayton smectite, F5 = Mount Binjour Green smectite, F6 = Hroznetin smectite.

near 716−720 cm^{-1}, which according to equation 2 can be assigned to Fe(II)Fe(II)-OH (Figure 4). The presence of bands near 718 and 760−770 cm^{-1} support assignment of at least a portion of the 818 cm^{-1} band to Fe(II) in some of these ferruginous smectites.

Table 3 shows the percentages of Fe(II) for each of the ferruginous smectites and nontronites determined by employing equation 3 to the best fits (Table 4) of the IR bending region. Given for comparison are the results from Mössbauer spectroscopy (Thomson *et al.*, 2007; Cashion *et al.*, 2008). None of the nontronites contains observable Fe(II).

Interestingly, the best fit for Drayton resulted in a rather broad band centered near 752 cm^{-1}, which is assigned here to MgMg-OH (see next section) and no assignment of an Fe(II) band could reasonably be made. Mössbauer spectroscopy (Johnston and Cardile, 1987; Cashion *et al.*, 2008) has shown that the Drayton

Table 3. Comparison of Fe(II) contents in ferruginous smectites as determined from IR spectra, as detailed in this paper, and derived from room-temperature Mössbauer spectra (Cashion *et al.*, 2008).

Smectite	% Fe(II) IR	% Fe(II) Mössbauer
Andamooka	11	n.m.
Redhill	14	10.5
Nibost	13	7
Drayton	nil	4
Mount Binjour Green	18	n.m.
Hroznetin	8	n.d.
Stebno	nil	n.d.
West Australia	nil	n.d.

n.m. – not measured
n.d. – not detected

smectite contains ~4% Fe(II) (Table 3). Also of interest is that the best decomposition of the IR spectrum of the Hroznetin smectite indicates that it contains ~8% Fe(II), but no Fe(II) was detectable in the room-temperature Mössbauer spectrum of this mineral (Table 3). These two samples reveal the uncertainties associated with the IR method, which perhaps over-estimates Fe(II) content by virtue of positioning peaks in the region of interest prior to minimizing the fit. However, the remarkable agreement for Fe(II) contents obtained from IR and Mössbauer spectra for the other ferruginous smectites studied here provide strong evidence in support of these assignments.

SPECTROSCOPIC EVIDENCE OF Mg BANDS IN FERRUGINOUS SMECTITES

Note that calculated positions for Fe(II)Mg-OH bands and MgMg-OH are separated by only a few wavenumbers (Table 1). The Nibost, Drayton, and Mount Binjour Green smectites have a band near 755 cm^{-1}, which can be assigned to either MgMg-OH or Fe(II)Mg-OH. There is, admittedly, a small probability of Mg-Mg nearest neighbors in the octahedral sheet of most dioctahedral smectites, as this would impart a large charge deficit. However, the high Mg contents of these three ferruginous smectites (~1 Mg cation per $O_{20}(OH)_4$ – Gates, 2005) indicate that such an assignment might be possible. As will be shown in the next section, in order for structural formula calculations based on IR spectra to match closely those from chemical analysis, assignment of most of this band to MgMg-OH sites is necessary.

Kaolin admixtures could result in some absorption bands in the region of interest that are not related to the assignments being made. Non-purified <2 μm fractions of Andamooka and Drayton smectites do indeed contain interstratifications of kaolin-smectite as well as illite-smectite. The Si-O bands of kaolin typically occur at 790, 755, and 697 cm^{-1} (Madejová and Komadel, 2001), and thus, bands near 750–760 cm^{-1} could be interpreted as being due to Si-O of kaolin. However, for Nibost and Mount Binjour Green smectites, no evidence of kaolin exists in XRD or in the OH-stretching region of the IR spectra (Figure 2; see also Gates, 2005). The Andamooka and Drayton smectites, which could conceivably have kaolin bands present in the OH-stretching region, do not have observable kaolin in the XRD (Figure 2). In addition, Andamooka has no band near 750–760 cm^{-1}. Thus, the Drayton smectite is the only sample in which a band near 755 cm^{-1} could possibly be associated with kaolin, but the intensity of this band and the large Mg content of this smectite provide strong support for the interpretation of the 755 cm^{-1} band being due to MgMg-OH.

Site occupancy in ferruginous smectites

Assuming that no admixtures exist in these samples (see Figure 2) and that the assignments of Fe(II) and Mg bands are correct, application of equation 3 enables reassignment of the octahedral site occupancies with respect to the presence of Fe(II) bands for the six

Table 4. OH-sharing octahedral cation-pair concentrations (normalized absorbance intensity) in five ferruginous smectites as determined from decomposition of the OH-bending region.

	Fraction of normalized absorbance					
	Andamooka	Redhill	Nibost	Drayton	Mount Binjour Green	Hroznetin
AlAl	0.545	0.388	0.307	0.289	0.208	0.405
AlFe(III)	0.206	0.215	0.275	0.367	0.287	0.308
Fe(III)Mg	0.122	0.275	0.131	0.115	0.217	0.114
Fe(III)Fe(III)	–	–	–	–	–	0.050
Al(Fe(II)	–	–	0.056	–	0.048	–
Fe(III)Mg	0.102	0.080	0.094	0.093	0.112	0.091
Fe(III)Fe(II)	0.010	0.033	–	–	0.026	0.017
MgMg	–	–	0.136	0.135	0.089	–
Fe(II)Mg	–	–	–	–	–	–
Fe(II)Fe(II)	0.015	0.010	–	–	0.011	0.015

Table 5. Octahedral cation distributions in six ferruginous smectites based on IR evidence for the presence of Fe(II) and Mg bands and the decompositions displayed in Figure 4 and Table 3. Also shown are distributions based on chemical analysis (CA) from Gates (2005) normalized to total cation occupancy of 4 per unit-cell.

Smectite	Analysis	Octahedral cations per $O_{20}(OH)_4$			
		Al	Fe(III)	Fe(II)	Mg
Andamooka	IR	2.83	0.64	0.08	0.45
	CA	2.88	0.67	–	0.44
Redhill	IR	2.53	0.66	0.11	0.71
	CA	2.49	0.77	–	0.74
Nibost	IR	2.15	0.75	0.11	1.00
	CA	2.16	0.86	–	0.98
Drayton	IR	2.12	0.92	0.00	0.96
	CA	2.05	0.96	–	1.00
Mount Binjour Green	IR	1.94	0.85	0.19	1.02
	CA	1.90	1.10	–	1.00
Hroznetin	IR	2.46	1.03	0.09	0.41
	CA	2.37	1.17	–	0.46

ferruginous smectites (Andamooka, Redhill, Nibost, Drayton, Mount Binjour Green, and Hroznetin). Recently, Vantelon *et al*. (2001) applied a similar technique to several montmorillonites, but the Fe(III) contents were considerably smaller in the smectites they studied.

Table 4 shows the results of decomposition of the bending region displayed in Figure 4 for six ferruginous smectites. Note that in Table 4, no assignments were made to Fe(II)Mg-OH. An assignment of MgMg-OH was chosen over Fe(II)Mg-OH, because of the large Mg content of these ferruginous smectites. If Fe(II)Mg-OH were used, the Mg contents derived using equation 3 would have been as much as 40% less than required to be in agreement with chemical data.

Table 5 shows the octahedral cation occupancy per unit-cell based on this analysis and compared to data given by Gates (2005) based on X-ray fluorescence (XRF) analysis of Ca^{2+}-saturated ignited samples. If the chemical analysis data are recast on an octahedral occupancy of 4, then the agreement between the two methods is quite good. Five of the six ferruginous smectites studied would have, however, a 6–17% increase in octahedral layer charge (Table 6). Two of the largest increases were for smectites where the Mg content required assignment of an MgMg-OH band (Nibost and Mount Binjour Green), but Drayton smectite, which also required MgMg-OH assignment, showed no difference in layer charge calculated by the two methods. Hroznetin smectite revealed a large difference due to the possible overestimation of Al from the AlAl-OH bands.

Figure 5 shows possible octahedral cation arrays for the six smectites based on the data discussed above. Note that for Nibost, Drayton, and Mount Binjour Green smectites, considerable MgMg clustering occurs. In developing these models, essentially all of the Mg in these three ferruginous smectites had to be clustered to simultaneously coincide with the IR data and structural formula displayed in Table 4. For the Andamooka, Redhill, Mount Binjour Green, and Hroznetin smectites, Fe(II) had to be clustered both with itself and with Fe(III), whereas this was not necessary for modeling Nibost smectite.

Octahedral Mg clustering in some smectites might be remnant chemical make-up related to incomplete weathering from Mg-enriched basalts (Velde, 1985; Weaver 1989). Differences in chemistries and weathering rates of the parent basalts may enable some smectites with larger Mg contents to occur locally. Available evidence for the Drayton smectite from Queensland, Australia, supports this concept as this clay occurs in soils (Drayton) formed on weathered basalts (Norrish and Tiller, 1976). This appears likely to also be the case for Mount Binjour Green smectite, which formed in partially weathered basaltic landscape (K. Norrish pers.

Table 6. Comparison of octahedral layer charge as determined from IR analysis and chemical analysis (CA) (Gates, 2005).

	Octahedral layer charge		
	IR	CA	%Diff
Andamooka	0.53	0.47	11
Redhill	0.79	0.74	6
Nibost	1.11	0.98	12
Drayton	0.96	0.97	1
Mount Binjour Green	1.21	1.00	17
Hroznetin	0.53	0.46	13

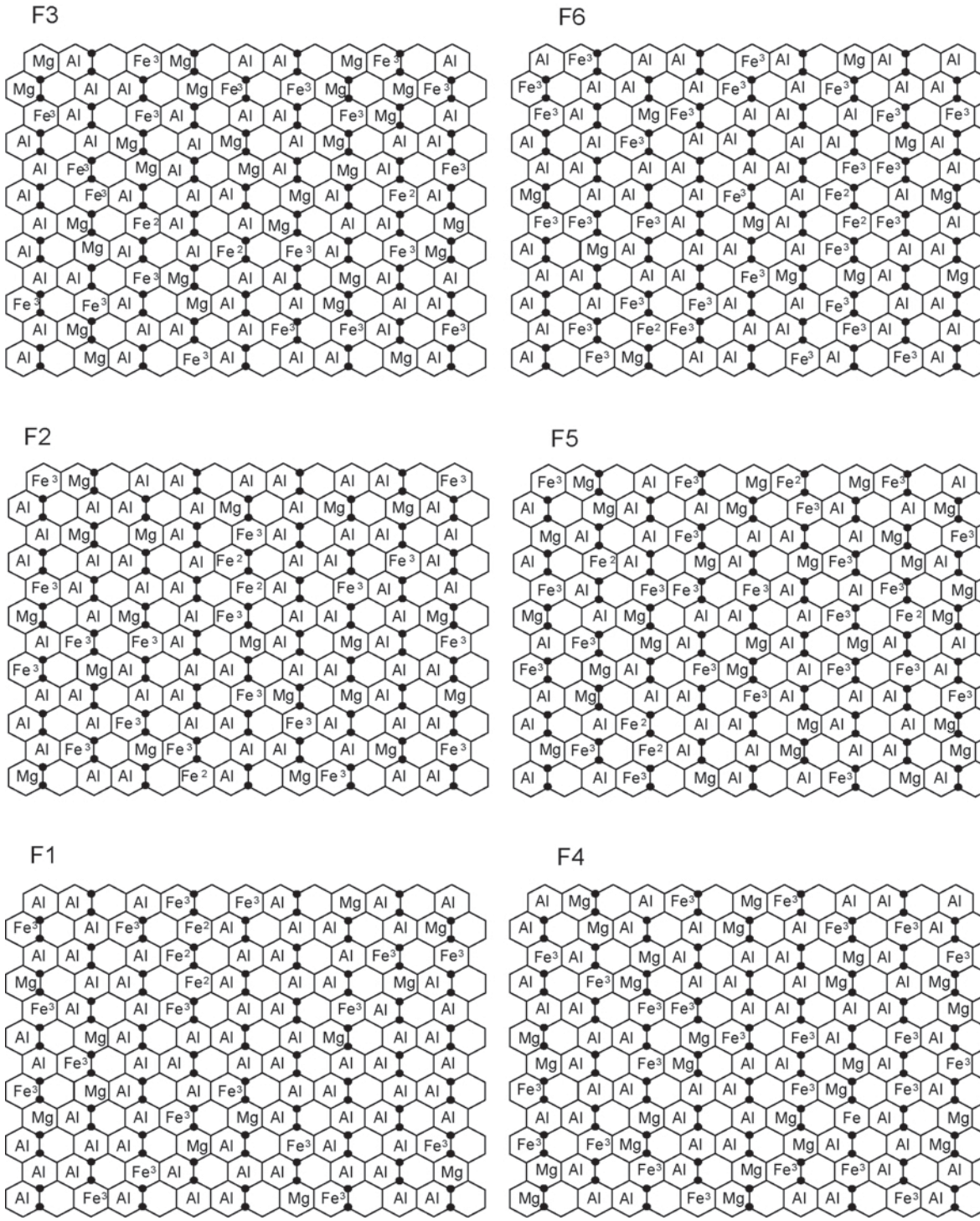

Figure 5. Possible cation arrangement in the octahedral sheet of some ferruginous smectites based on structural chemistry and IR data.

comm., 2007; Teakle, 1952; Beckmann *et al.*, 1974). However, for the Nibost smectite, from the Isle of Skye, UK, the evidence is less clear, as no information as to the exact locality and parent material are known. Skye has substantial surface basalt (mafic), and many smectites (predominantly saponites) are known to derive from the basalts (M.J. Wilson pers. comm., 2007; S. Hillier pers. comm., 2007).

The stability of MgMg clustering within the octahedral array may be related to the distribution of both tetrahedral Al and MgMg pairs such that the charge deficit is as widely distributed across the 2:1 layers as possible. Again, the best evidence in support is for the Drayton smectite (Norrish and Tiller, 1976) where the high layer charge, predominantly located in the tetrahedral sheet, was shown to be responsible for the subplastic (inability to disperse) behavior of these clays (Butler, 1976). It was postulated that the clays, being formed in place, are in a "state of incomplete weathering" (Norrish and Tiller, 1976). The high layer charge of the Mount Binjour Green smectite (also from Queensland basalt) is attributed largely to the Mg content (Table 6), and Mg clustering would result in a strong field of charge emanating from the interlayer surface. A uniform distribution, where all charge points are separated by as great a distance as possible, should make such a structure more stable, especially when the tetrahedral charge contribution is high, as in Nibost and Drayton. The Mount Binjour Green smectite has the greatest extent of Mg clustering (Figure 5), but also the smallest contribution of tetrahedral layer charge of these three smectites. For other smectites (the normal case), perhaps clay genesis occurs at a temperature, pH, and other conditions where MgMg clustering is unstable (Velde, 1985; Weaver, 1989).

Band assignments in nontronites

Within the nontronites, when octahedral Fe(III) exceeds 3.5 per unit cell, the OH-bending region of the IR spectra is more representative of the end-member nontronite (Goodman *et al.*, 1976; Gates, 2005). The main features are an Fe(III)Fe(III)-OH doublet centered near 844 and 817 cm^{-1} and the Fe-O out-of-plane deformation near 676 cm^{-1} (Figure 6). The presence of the doublet Fe(III)Fe(III)-OH band is diagnostic for nontronite (Gates, 2005) as the ferruginous smectites lack this doublet and instead have a single band centered near 818 cm^{-1}. As expected, none of the 14 nontronites studied by Gates (2005) and Gates *et al.* (2002) have discernible Fe(II) as measured by Mössbauer spectroscopy (Table 3, Cashion, 2007, unpublished results).

Differences in the intensities of the two Fe(III)Fe(III)-OH bands in nontronite are reflected in the amount of tetrahedral Fe(III) (Gates *et al.*, 2002). The ratio of the 844 to 817 cm^{-1} band is positively correlated ($r = 0.952$) to the tetrahedral Fe(III) to octahedral Fe(III) ratio. Nontronites with nil tetrahedral Fe(III), *e.g.* Cheney (Figure 6), show minimal development of the 844 cm^{-1} band, but for nontronites with greater total Fe(III) contents this band increases in intensity with increasing proportion of tetrahedral Fe(III) (Figure 6, Gates *et al.*, 2002), despite no consistency with tetrahedral layer charge.

The presence of an AlMg-OH band is indicative of montmorillonites and ferruginous smectites with <12% Fe_2O_3, with those having >12% Fe_2O_3 showing increased Fe(III)Mg-OH band intensity. The IR spectra of ferruginous smectites having >18% Fe_2O_3 and nontronites with <37% Fe_2O_3 studied by Gates (2005) can be decomposed (Figure 6) to have a broad band near 750−760 cm^{-1}. Application of equation 2 would indicate assignment of this band as Fe(III)Fe(II)-OH, Fe(II)Mg-OH, or MgMg-OH. As Fe(II) can be ruled out in the nontronites, MgMg-OH is a probable assignment, and it implies that most nontronites probably have Mg-Mg clustering as depicted for some of the ferruginous smectites shown in Figure 5.

The intensities of the 750−760 cm^{-1} band and that for Fe(III)Mg-OH near 785 cm^{-1} are generally greater for those nontronites having >0.2% MgO. For end-member nontronites, and those with <0.2 MgO, the band near 750−760 cm^{-1} is absent (Gates, 2005). The Mg content of these nontronites ranges from 0.03 to 0.28 per unit cell, so the intensity seems excessive to account for the Mg content. Since octahedral Mg is the sole source of octahedral charge in nontronites, the absorption coefficient of the OH associated with Mg may be strongly affected, thereby increasing the intensity of the Fe(III)Mg-OH band. Even for the three ferruginous smectites (Stebno, West Australian, and SWa-1) with 0.25−0.5 Mg per unit cell, the band intensity is high.

Another plausible explanation is that in the nontronites the band near 750−760 cm^{-1} may be associated with a nontronite Si-O band (Goodman *et al.*, 1976). For example, in the Uley brown nontronite, NAu-2, a band near 755 cm^{-1} is well resolved (Gates, 2005), and this sample also shows a band near 724 cm^{-1}, which, in combination with a portion of the 790 cm^{-1} band, could be associated with Si-O in ribbon silicates (Strens, 1974). The Uley brown nontronite was shown to derive from weathered amphibolite, and minerals of this group were observed in coarse fractions (Keeling *et al.,* 2000). Nontronite crystallites like NAu-2 often have lath-like morphology, and this nontronite is believed to have formed in association with the parent minerals (Keeling *et al.*, 2000). Thus, the octahedral occupancy may be constrained by the original mineral structure/morphology relationship (Janney and Banfield, 1998).

CONCLUSIONS

Positions of OH-bending vibrations for dioctahedral smectites follow the same relationship as determined by Besson and Drits (1997a) for the OH-sharing stretching vibrations in micas. The cation mass-valence sum (CM-VS) relationship was used to enable assignment of OH-sharing octahedral Mg and Fe(II), which have not been assigned previously. Ferruginous smectites having between 7 and 13% Fe_2O_3 (ignited basis) seem to have the greatest assortment of Fe(II) cations, including bands associated with AlFe(II)-OH, Fe(III)Fe(II)-OH, Fe(II)Mg-OH, and Fe(II)Fe(II)-OH. Some ferruginous smectites also have considerable Mg-Mg clustering,

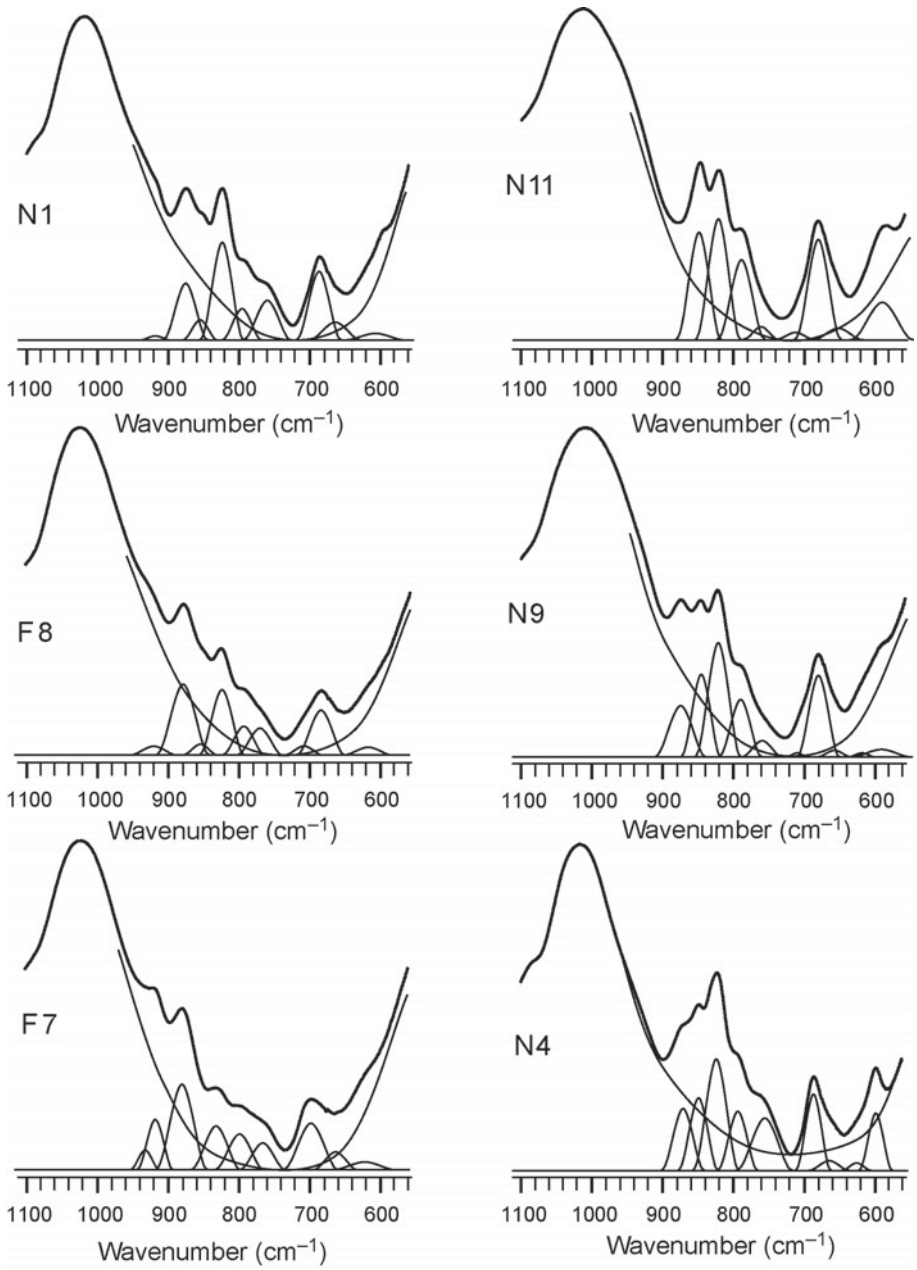

Figure 6. Decomposition of the OH-bending region of IR spectra of some ferruginous smectites and nontronites detailing the bands associated with true nontronites. F7 = Stebno smectite, F9 = SWa-1 ferruginous smectite, N1 = Cheney nontronite, N4 = NAu-1 Uley nontronite, N8 = NG-1 Hohen Hagen nontronite, N11 = Spokane nontronite.

resulting in assignment of MgMg-OH bands. Without this assignment, Mg occupancies calculated from the IR data are under-represented by as much as 40%.

Thirty one of the 35 smectites studied by Gates (2005) had a band near 785−795 cm^{-1} definitively assigned to Fe(III)Mg-OH bending. This band is associated with another band near 750−760 cm^{-1} in ferruginous smectites and nontronites having between 18 and 37% Fe_2O_3, which is related to Mg content. Absorption bands associated with Fe(II) and Mg in dioctahedral smectites are low in intensity, but in nontronites and some ferruginous smectites their normalized absorbance intensities are greater than chemistry suggests. This is interpreted as indicating that Mg-Mg clustering, where the Mg shares OH, probably occurs.

ACKNOWLEDGMENTS

Collection of IR data for this work was conducted while the author was employed by CSIRO Land and Water (Australia).

REFERENCES

Beckmann, G.G., Thompson, C.H., and Hubble, G.D. (1974) Genesis of red and black soils on basalt on the Darling Downs, Queensland, Australia. *European Journal of Soil Science*, **25**, 265–281.

Besson, G. and Drits, V.A. (1997a) Refined relationship between chemical composition of dioctahedral fine-grained mica minerals and their infrared spectra within the OH stretching region. Part 1. Identification of the OH stretching vibrations. *Clays and Clay Minerals*, **45**, 158–169.

Besson, G. and Drits, V.A. (1997b) Refined relationship between chemical composition of dioctahedral fine-grained mica minerals and their infrared spectra within the OH stretching region. Part 2. Main factors affecting OH vibrations and quantitative analysis. *Clays and Clay Minerals*, **45**, 170–183.

Bishop, J.L., Murad, E., Madejová, J., Komadel, P., Wagner, U., and Scheinost, A.C. (1999) Visible, Mössbauer, and infrared spectroscopy of dioctahedral smectites: structural analysis of the Fe-bearing smectites, Sampor, SWy-1, and SWa-1. Pp. 413–419 in: *Clays for Our Future* (H. Kodoma, A.R. Mermut and J.K. Torrence, editors). Proceedings of the 11th International Clay Conference, Ottawa, Canada.

Botella, V., Timon, V., Escamilla-Rosa, E., Hernandez-Languna, A., and Sainz-Diaz, C.I. (2004) Hydrogen bonding and vibrational properties of hydroxyl groups in the crystal lattice of dioctahedral clay minerals by means of first principles calculations. *Physics and Chemistry of Minerals*, **3**, 475–486.

Butler, B.E. (1976) Subplasticity in Australian soils. Introduction. *Australian Journal of Soil Research*, **14**, 225–226.

Cashion, J.D., Gates W.P., and Thomson, A. (2008) Mössbauer and IR analysis of iron sites in four ferruginous smectites. *Clay Minerals*, in press.

Čicel, B., Komadel, P., Bednáriková, E., and Madejová, J. (1992) Mineralogical composition and distribution of Si, Al, Fe, Mg and Ca in the fine fractions of some Czech and Slovak bentonites. *Geologica Carpathica, Series Clays*, **43**, 3–7.

Drits, V.A. and Manceau, A. (2000) A model for the mechanism of Fe^{3+} to Fe^{2+} reduction in dioctahedral smectites. *Clays and Clay Minerals*, **48**, 185–195.

Dong, H.L., Kostka, J.E., and Kim, J. (2003) Microscopic evidence for microbial dissolution of smectite. *Clays and Clay Minerals*, **51**, 502–512.

Fialips, C.I., Huo, D., Yan, L., Wu, J., and Stucki, J.W. (2002a) Effect of oxidation state on the IR spectra of Garfield nontronite. *American Mineralogist*, **87**, 630–641.

Fialips, C.I., Huo, D., Yan, L., Wu, J., and Stucki, J.W. (2002b) Infrared study of reduced and reduced-reoxidized ferruginous smectite. *Clays and Clay Minerals*, **50**, 455–469.

Gates, W.P. (2005) Infrared spectroscopy and the chemistry of dioctahedral smectites. Pp. 125–168 in: *Vibrational Spectroscopy of Layer Silicates and Hydroxides* (T. Kloprogge, editor). CMS Workshop Lecture Series Vol. **13**, The Clay Minerals Society, Chantilly, Virginia, USA.

Gates, W.P., Slade, P.G., Manceau A., and Lanson, B. (2002) Site occupancy by iron in nontronite. *Clays and Clay Minerals*, **50**, 223–239.

Goodman, B.A., Russell, J.D., Fraser, A.R., and Woodhams, F.W.D. (1976) A Mössbauer and I.R. spectroscopic study of the structure of nontronite. *Clays and Clay Minerals*, **24**, 53–59.

Heller-Kellai, L. (1997) Reduction and reoxidation of nontronite: the data reassessed. *Clays and Clay Minerals*, **45**, 476–479.

Janney, D.E. and Banfield, J.F. (1998) Distribution of cations and vacancies and the structure defects in oxidized intermediate olivine by atomic-resolution TEM and image simulation. *American Mineralogist*, **83**, 799–810.

Johnston, J.H. and Cardile, C.M. (1987) Iron substitution in montmorillonite, illite, and glauconite by ^{57}Fe Mössbauer spectroscopy. *Clays and Clay Minerals*, **35**, 170–176.

Keeling, J.L., Raven, M.D., and Gates, W.P. (2000) Geology and preliminary characterization of two hydrothermal nontronites from weathered metamorphic rock at the Uley graphite mine, South Australia. *Clays and Clay Minerals*, **48**, 105–110.

Kim, J., Dong, H.L., Seabaugh, J., Newell, S.W., and Eberl, D.D. (2004) Role of microbes in the smectite-to-illite reaction. *Science*, **303**, 830–832.

Komadel, P., Stucki, J.W., and Čícel, B. (1993) Readily HCl-soluble iron in the fine fractions of some Czech bentonites. *Geologica Carpathica, Series Clays*, **44**, 11–16.

Komadel, P., Madejová, J., and Stucki, J.W. (1995) Reduction and reoxidation of nontronite – questions of reversibility. *Clays and Clay Minerals*, **45**, 105–110.

Lear, P.R. and Stucki, J.W. (1985) The role of structural hydrogen in the reduction and reoxidation of iron in nontronite. *Clays and Clay Minerals*, **33**, 539–545.

Lear, P.R., Komadel, P., and Stucki, J.W. (1988) Mössbauer spectroscopic identification of iron oxides in nontronite from Hohen Hagen, Federal Republic of Germany. *Clays and Clay Minerals*, **36**, 376–378.

Lee, I., Kostka, J.E., and Stucki, J.W. (2006) Comparison of structural Fe reduction in smectites by bacteria and dithionite: an infrared spectroscopic study. *Clays and Clay Minerals,* **54**, 195–208.

Madejová, J. and Komadel, P. (2001) Baseline studies of the Clay Minerals Society Source Clays: infrared methods. *Clays and Clay Minerals*, **49**, 410–432.

Madejová, J., Komadel, P., and Číčel, B. (1994) Infrared study of octahedral site populations in smectites. *Clay Minerals*, **29**, 319–326.

Martinez-Alonso, S., Rustad, J.R., and Goetz, A.F.H. (2002) Ab initio quantum mechanical modelling of infrared vibrational frequencies of the OH group in dioctahedral phyllosilicates. Part 1: Methods, results and comparison to experimental data. *American Mineralogist*, **87**, 1215–1223.

Norrish, K. and Tiller, K.G. (1976) Subplasticity in Australian soils. V. Factors involved and techniques of dispersion. *Australian Journal of Soil Research*, **14**, 273–289.

Petit, S., Caillaud, J., Righi, D., Madejová, J., Elsass, F., and Köster, H.M. (2002) Characterisation and crystal chemistry of a Fe-rich montmorillonite. *Clay Minerals*, **37**, 283–297.

Slonimskayá, M.V., Besson, G., Dainyak, L.G., Tchoubar, C., and Drits, V.A. (1986) Interpreation of the IR spectra of celadonites and glauconites in the region of OH-stretching frequencies. *Clay Minerals*, **21**, 115–149.

Strens, R.G.J. (1974) The common chain, ribbon and ring silicates. Pp. 305–330 in: *The Infrared Spectra of Minerals* (V.C. Farmer, editor). Monograph **4**, Mineralogical Society, London.

Stucki, J.W. and Kostka, J.E. (2006) Microbial reduction of iron in smectites. *Comptes Rendus Geoscience*, **338**, 468–475.

Stucki, J.W. and Roth, C.B. (1976) Interpretation of the infrared spectra of oxidized and reduced nontronite. *Clays and Clay Minerals*, **24**, 293–296.

Teakle, L.J.H. (1952) An interpretation of the occurrence of diverse types of soils on basalt in Northern NSW and Queensland. *Australian Journal of Agricultural Research*, **3**, 391–408.

Thomson, A., Cashion, J.D., and Gates, W.P. (2007) Mössbauer analysis of iron sites in four Na- and Ca-

saturated ferruginous smectites. *Proceedings of the 31st Australia and New Zealand Condensed Matter and Materials Meeting*, Wagga Wagga, New South Wales, Australia. http://www.aip.org.au//wagga2007/2007_29.pdf

Vantelon, D., Pelletier, M., Michot, L.J., Barres, O., and Thomas, F. (2001) Fe, Mg and Al distribution in the octahedral sheet of montmorillonites. An infrared study in the OH-bending region. *Clay Minerals*, **36**, 369–379.

Velde, B. (1985) *Clay Minerals. A Physico-chemical Explanation of their Occurrence*. Developments in Sedimentology, **40**, Elsevier, Amsterdam, 427 pp.

Weaver, C.E. (1989) *Clays, Muds and Shales*. Developments in Sedimentology, **44**. Elsevier, Amsterdam, 819 pp.

(*Received 22 March 2007; revised 8 August 2007; Ms. 0001; A.E. P. Komadel*)